Selection of Mass Transfer Models for Competitive Adsorption of Antibiotics Mixture from Aqueous Solution on Delonix regia Pod Activated Carbon

[1,2]Ayobami O. Ajani, [1,2,3]Ilesanmi A. Ojo, [1,2]Wasiat O. Bello, [1,2,3]Ameen N. Akinsola,
[1,2]Tinuade J. Afolabi, and *[1,2,4]Abass O. Alade

[1] Department of Chemical Engineering, Ladoke Akintola University of Technology, Ogbomoso, Nigeria
[2] Bioenvironmental, Water and Engineering Research Group, Ladoke Akintola University of Technology, Ogbomoso, Nigeria
[3] Science Laboratory Unit, Faculty of Natural and Applied Sciences, Al-Hikmah University, Ilorin, Nigeria
[4] Science and Engineering Research Group, Ladoke Akintola University of Technology, Ogbomoso, Nigeria
{aoajani|tjafolabi|aoalade}@lautech.edu.ng|{iaojo|anakinsola}@alhikmah.edu.ng|wobello@pgschool.lautech.edu.ng

ORIGINAL RESEARCH

Abstract- The selection of suitable mass transfer models that fit the adsorption of a mixture of antibiotics in aqueous solution onto activated carbon derived from Delonix Regia Pods (DRPs) was examined in this study. The ripe DRPs were cleaned, activated with KOH and then carbonised at 350 °C. The surface chemistry of the raw and the modified DRPs were characterised using Fourier Transform Infrared (FTIR), before being subjected to batch adsorption of a mixture of Amoxicillin (AMO), Tetracycline (TETRA) and Ampicillin (AMP) under the effect of time (0-240 mins), and concentration (20-100 mg/l). The adsorption diffusion mechanisms of the process were analysed. The spectra of the raw and modified DRP indicate the existence of hydroxyl groups alkanes, unconjugated ketone, carbonyl, and ester groups. McKay has the highest R^2 (0.9445) for the mass transfer diffusion model. This indicates that the adsorption rate of the selected antibiotics in the wastewater is regulated and monitored by the internal mass transport processes in accordance with a pore diffusion mechanism.
.
Keywords- Antibiotics, Adsorbent, Delonix regia, Diffusion model, wastewater.

———————————— ◆ ————————————

1 INTRODUCTION

The advancement of pharmaceutical industries has to the production of varieties of drug products and antibiotics have recorded an upsurge in demand and consumption by humans and animals. The antibiotics are usually consumed in excess and the unmetabolized quantity is being excreted into the ecosystem and surface waters being the receivers. This phenomenon usually led to the occurrence of antibiotic-resistant strains of microorganisms, which impair the food web system thereby causing harm to the aquatic lives, animals and humans (Mohammed *et al.,* 2022).

Antibiotics such as tetracycline, ampicillin, and amoxicillin are largely used in modern industrial livestock operations and used and expired drugs are carelessly discharged into the environment without proper treatment. Large concentrations are used in livestock and poultry farms (where antibiotics typically are fed to healthy animals for disease prevention), which generate an enormous amount of wastewater often containing undigested antibiotics. It is estimated that as much as 80-90 % of all antibiotics given to humans and animals are not fully broken down and are eventually released into the environment (Barbooti and Zahraw 2020).

Antibiotic usage increased rapidly and concerns focused on their residues in the aquatic environment have become a global problem posing a serious threat to the environment and an inherent health risk to human beings (Azarpira et al. 2019). Various treatment techniques employable for the r the removal of antibiotics from wastewater streams include, biodegradation, membrane filtration, ozonation, and, reverse osmosis (Amuda *et al.,* 2015), however, their efficacies are challenged by economic and technical feasibilities (Amole *et al.,* 2021). The choice of adsorption technique has been welcomed in many studies due relative higher efficiency in removing dissolved organics (Amole *et al.,* 2021). There is, therefore, a growing interest in novel and low-cost adsorbents. One of the important factors often investigated in understating the characteristics of adsorption is kinetic studies.

Kinetics studies of the adsorption process are employed to decide and establish the adsorption rate mechanisms and the possible rate that controls the adsorption process (Revellame et al. 2020). The general adsorption process used to determine the mechanism of adsorbate(s) onto selected adsorbent is assumed to occur using a three-step model, which is (i) mass transfer of adsorbate from the bulk solution to the adsorbent surface, (ii) adsorption of adsorbate onto sites and (iii) internal diffusion of adsorbate through either a pore diffusion model or a homogeneous solid-phase diffusion model (Amole *et al.,* 2021). The basic principle behind the rate of adsorption mechanisms involves the search for the best model that best fits the data generated. Consequently, some important variables such as equilibrium time, mechanism of adsorption and the rate-determining step can be determined (Supriyadi et al. 2019). However, the main objective of this study was to examine the transfer mechanism that occurs in the adsorption of a mixture of

---

pollutants, particularly antibiotics mixture (amoxicillin ampicillin and tetracycline), which are involved in a competition for the available surface and pore of the adsorbent.

2 MATERIALS AND METHODS
2.1 SAMPLE COLLECTION AND MATERIAL PREPARATION

Mature raw *Delonix Regia* pod samples obtained from flamboyant trees planted at Mandate Estate, Ilorin, Kwara State, Nigeria were washed, rinsed thoroughly and then sundried (Amuda et al. 2015). They were further oven-dried, milled to uniform particle size (425-850 μm). and activated with KOH by impregnating the DRP sample (10 g) in 100 ml of 1.0 M KOH at room temperature for 24 h in a 500 ml beaker (Dada et al. 2020). The excess solution was boiled off and the paste formed was cooled, washed with distilled water and treated with 0.1 M HCL to adjust the pH to 7.0±0.1. The activated DRP sample was oven-dried at 105 °C overnight and then carbonised at 500 °C in a muffle furnace for 40 min (Ravichandran et al. 2018). The surface chemistry of the raw and carbonised DRP sample was characterised by Fourier Transform Infrared Spectrophotometer according to (George et al. 2014). The DRP samples were mixed with KBr and placed in the sample holder to get the spectra within the range of 4000 to 400 cm^{-1} on the FTIR spectrometer which was operated at 200 scans per sample and 4 cm^{-1} resolution (George et al. 2014).

2.2 BATCH ADSORPTION STUDIES

The aqueous solution (100 ml) containing 20-100 mg/L of the mixture of selected antibiotics (amoxicillin ampicillin and tetracycline) in the equal ratio was treated with 1 g of DRPAC in a 250 ml flask at room temperature, at 180 rpm and varying the contact time (10 and 240 mins) (Mashkour 2012). The supernatant of the treated solution was decanted carefully and subjected to UV-VIS spectrophotometry at 287, 288 and 361 nm for amoxicillin ampicillin and tetracycline respectively (Rahmanian et al. 2018).

2.3 MASS TRANSFER DIFFUSION MODELS

The mass transfer diffusion models were considered for the understanding of feasible diffusion mechanisms in the adsorption of selected antibiotics mixture on the DRPAC developed. The Weber Morris Intraparticle diffusion model involves pore diffusion where adsorbate molecules percolate into the interior of adsorbent particles and are used to estimate and determine the rate of the adsorption process (Supriyadi et al. 2019). The Matthew-Weber transfer diffusion model is used to examine the external mass transfer on the boundary phase around the adsorbent understudy (Supriyadi et al. 2019). The Banghams transfer diffusion model is used to decide and actuate the influence of the pore diffusion on the rate-limiting step of the transfer diffusion (Benjelloun et al. 2021). The McKay film transfer diffusion also known as surface diffusion is another adsorption mechanism where the adsorbate is transported from the region of higher concentration to the external surface of the adsorbent. It involves a mass transfer, which is based on film diffusion. The model equations for the mass transfer diffusion models and the parameters that were plotted against each other in order to construe the models' constants are stated in Table 1.

Table 1. Mass Transfer Diffusion Models

Models	Models Equation	Plot
Weber-Morris	$q_t = k_{wm}\ t^{0.5} + C$	q_t against $t^{0.5}$
Matthew-Weber	$\log \frac{C_t}{C_0} = -\frac{K_m A}{2,303}\ t$	$\log \frac{C_t}{C_0}$ against t
Banghams	$\log\left(\log \frac{C_0}{C_0 - q_t.m}\right) = \log\left(\frac{k_b.m}{2.303.V}\right) + \theta \log t$	$\log\left(\log \frac{C_0}{C_0 - q_t.m}\right)$ against log t
McKay film	$\ln(1 - F) = -k_m t$	$\ln(1-F)$ against t $(F = \frac{q_t}{q_e},)$

Where k_{wm} (mg/gmin$^{0.5}$) is the intra-particle diffusion rate constant and C (mg/g) is proportional to the boundary layer thickness. c_t and c_o are the adsorbate concentration at time t and the initial solute concentration (mg/g), k_m is the external mass transfer coefficient (m/h) and A is the external surface per unit mass (m²/g). V is the volume of the liquid phase, m is the weight of adsorbent per litter of solution g/l, and k_b and $\theta < 1$ are constants. K_m is the diffusion rate constant; F is the adsorption capacity and is gotten as $\frac{q_t}{q_e}$, q_t is the adsorption capacity at each time and q_e is the adsorption capacity at equilibrium.

3 RESULTS AND DISCUSSION
3.1 FOURIER TRANSFORM INFRARED ANALYSIS OF THE SAMPLES

The spectra of the FTIR analysis of the raw DRP are shown in Figure 1a. It showed the presence of broad absorption peaks at 3450.29 cm^{-1}, 2925.43 cm^{-1}, 1750.55 cm^{-1}, 1608.50 cm^{-1}, 1608.50 cm^{-1}, 1360.96 cm^{-1} and 897.63 cm^{-1} (Table 2), which indicate the presence of O–H stretching vibration, saturated CH$_2$ stretching vibration substitution bond, C=C stretching vibration, C=C stretching vibration, aromatic skeletal vibrations, and C-O stretching vibrations linked to hydroxyl, alkanes, unconjugated ketone, carbonyl and ester, carbonyl, alkenes and ester,

aromatic ring, carbonyl and alkenes, benzene ring, aromatic hydrocarbons, cellulose as well as aldehyde, respectively. The FTIR of carbonized DRP (Figure 1b) showed the presence of broad absorption peaks at 3500.01 cm^{-1}, 2973.17 cm^{-1}, 850.70 cm^{-1}, 1750.55 cm^{-1}, 1618.37cm^{-1} 1497.21 cm^{-1}, 1250.49 cm^{-1}, 1360.98 cm^{-1} and 1025.01 cm^{-1} (Table 2), which indicate shift from the peak position on the raw DRP sample (Figure 1). This development suggested that the selected activant (KOH) might have interfered with the surface chemistry of the *Delonix regia* pod adsorbent (Seshadri *et al.* 2012).
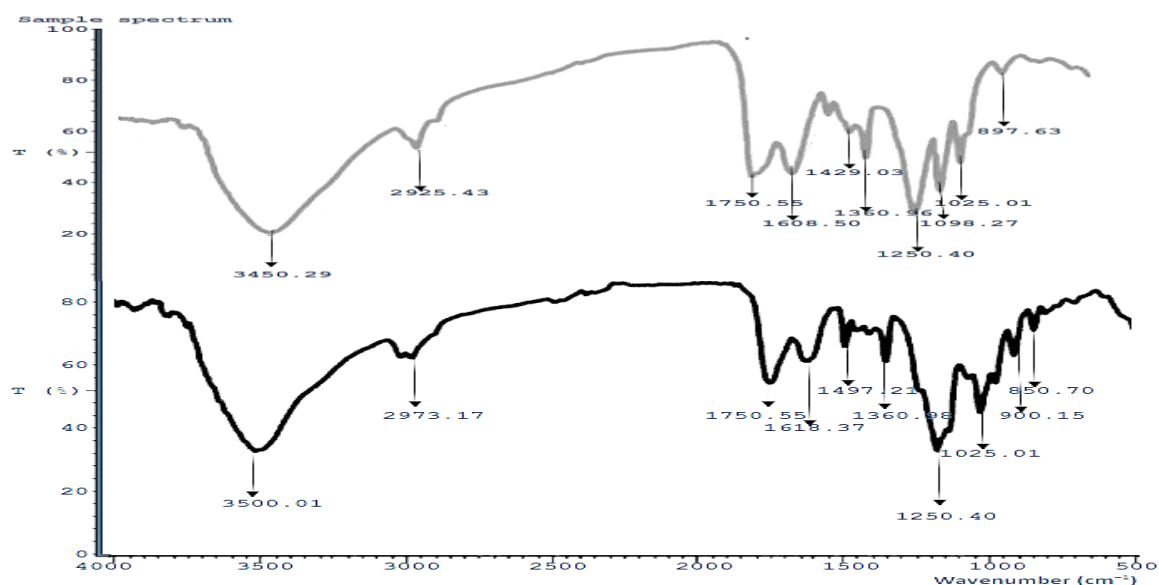
Fig. 1: FTIR spectra of (a) raw sample of DRP and (b) carbonized sample of DRP

Table 2. FTIR spectra of raw sample and carbonized sample of DRP

Raw Sample				Carbonized Sample			
Peak (cm^{-1})	Transmittance (%)	Bond type	Functional group	Peak (cm^{-1})	Transmittance (%)	Bond type	Functional group
3450.29	32.61	O–H	Hydroxyl	3500.01	33.70	O-H	Hydroxyl
2925.43	64.00	CH$_2$	Alkanes	2973.17	64.00	C–H	Alkanes
1750.55	55.72	C=C	CAE	1750.55	53.81	C=C	CAE
1608.50	64.38	C=C	CA	1618.37	65.98	N–H	Amine
1429.03	67.21	BR	AH	1497.21	68.09	C=O	Carbonyl
1360.96	61.80	C-O	Aldehyde	1360.98	64.72	C-O	Aldehyde
1250.40	32.05	C=C	Carbonyl	1250.49	33.51	C–O–C	Carboxyl
1098.27	44.00	C–O	Aldehyde	1025.01	44.18	C–O	Aldehyde
1025.01	64.26	C–H	Alkenes	900.15	65.22	C–H	Alkenes
897.63	74.00	Cellulose	Aldehyde	850.70	70.30	C–H	Alkanes

CAE-Carbonyl, Alkenes and Ester; CA-Carbonyl and Alkenes; AH-Aromatic Hydrocarbons, BR-Benzene ring

3.2 BATCH ADSORPTION OF SELECTED ANTIBIOTICS MIXTURE ONTO DRPAC DEVELOPED

The trends of adsorption capacity for the increase in time and initial concentration indicates that the maximum adsorption capacity at 20 mg/L (1.7871, 1.6364 and 1.600 mg/g), 40 mg/L (3.732, 3.500 and 3.400 mg/g), 60 mg/L (3.656, 5.409 and 5.200), 80 mg/L (7.496, 7.295 and 6.867) and 100 mg/L (9.371, 9.31 and 8.733 mg/g) were obtained for AMO, TETRA and AMP respectively. The general order of affinity for the pollutants is TETRA > AMO >AMP which showed an exceptional relationship with their molecular weight of 444.4, 365.4 and 349.4, respectively.

3.3 MASS TRANSFER DIFFUSION

The mass transfer diffusion of this study was examined using the Weber-Morris, Matthew-Weber, Bangham and McKay film diffusion models (Figures 2-5).

3.3.1 Weber-Morris Diffusion Model

The value of K_{wm} were in the range of 0.1098-0.5095, 0.1150-0.4359, and 0.1113-0.4576 mgg^{-1}min$^{-0.5}$ for amoxicillin, tetracycline and ampicillin, respectively, and increased as the concentration increased from 20 to 100 mg/L (Table 3). This suggests the occurrence of multiple adsorption stages. Their corresponding values of C were in the range 0.3260-3.6126, 0.4991-4.8564, and 0.2485-3.6671 mg/g. These values reflect the boundary layer effect which suggested a larger contribution of the surface to the rate-determining step (Dada *et al.* 2016). However, since the plot of qt versus t$^{0.5}$ did not pass through the origin thus intraparticle diffusion was not the sole rate-determining step (Dada *et al.* 2016).

3.3.2 Matthew-Weber Diffusion Model

The values of K_{mw} decreased from 0.3915 to 0.1612, 0.2994 to 0.0461 and 0.4376 to 0.1383 mg/g.min for amoxicillin, tetracycline and ampicillin respectively (Table 3), as the concentration increased from 20 to 100 mg/L. The trend shows an inverse relationship with the increasing temperature, and this is not expected because the model equation displays a direct relationship of its parameters, thus can be suggested that this model is not suitable for the adsorption process (Oyelowo *et al.* 2020).
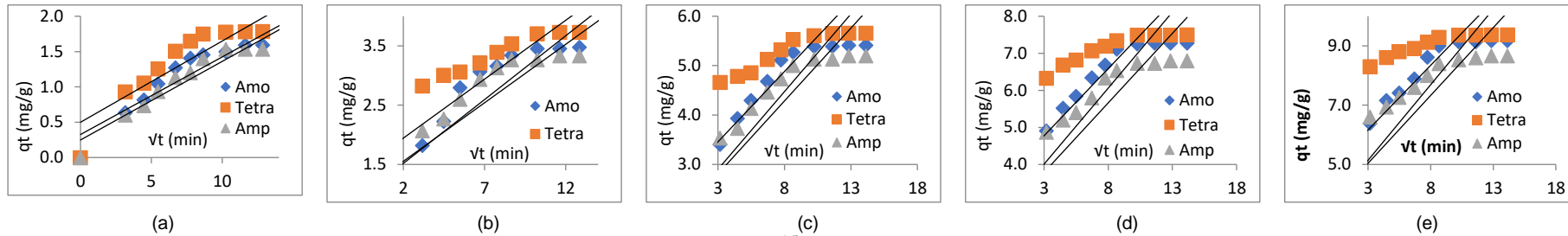
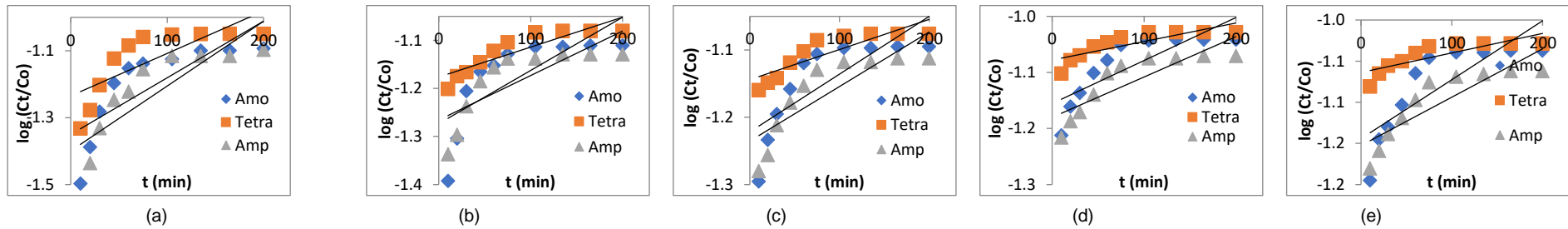Fig. 2: Weber-Morris plot of q_t against $t^{0.5}$ for (a) 20, (b) 40, (c) 60, (d) 80 and (e) 100 mg/L

Fig. 3: Matthew-Weber plot of q_t against t^0.5 for (a) 20, (b) 40, (c) 60, (d) 80 and (e) 100 mg/L

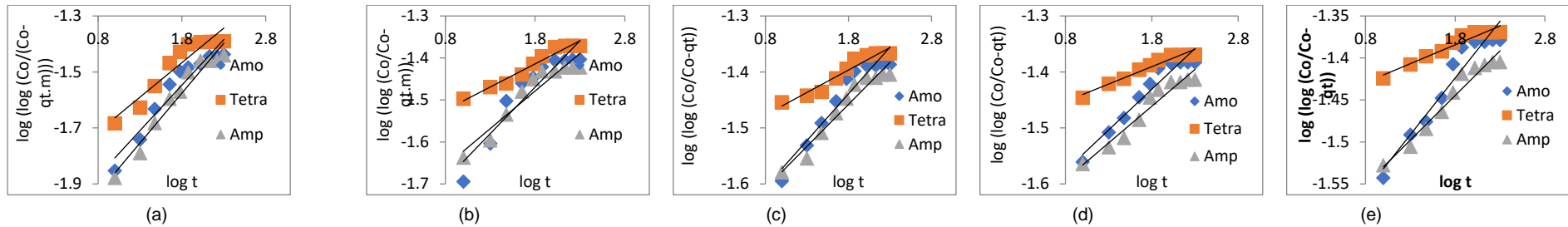

Fig. 4: Bang ham plot of log (log $\frac{C_0}{C_0 - q_t.m}$) against log t for (a) 20, (b) 40, (c) 60, (d) 80 and (e) 100 mg/L
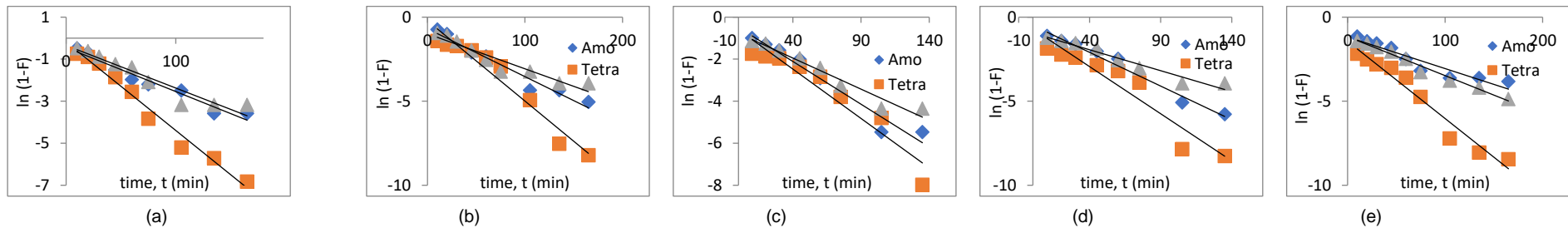

Fig. 5: McKay film diffusion plot of q_t against $t^{0.5}$ for (a) 20, (b) 40, (c) 60, (d) 80 and (e) 100 mg/L

Table 3. Evaluated parameters of the Selected diffusion Models at different concentrations of the selected antibiotic mixtures

Conc. (mg/L)		Weber-Morris			Matthew-Weber		Bangham			McKay	
		K_{wm} (mg/g $min^{0.5}$)	C (mg/g)	R^2	K_m (mg/g .min)	R^2	k_b (mL/ g/L)	θ	R^2	k_m	R^2
20	AMO	0.1098	0.3260	0.867	0.3915	0.624	1.6998	0.3250	0.920	0.0209	0.961
	TETR	0.1150	0.4991	0.798	0.2994	0.604	2.8320	0.2464	0.900	0.0421	0.978
	AMP	0.1113	0.2485	0.912	0.4376	0.703	1.3986	0.3562	0.955	0.0203	0.915
40	AMO	0.2153	1.0872	0.761	0.2533	0.555	3.1224	0.2213	0.878	0.0285	0.958
	TETR	0.1987	1.5469	0.640	0.1382	0.790	5.6220	0.1102	0.961	0.0478	0.946
	AMP	0.1973	1.1588	0.729	0.2073	0.612	3.6399	0.1790	0.905	0.0208	0.906
60	AMO	0.3144	1.9585	0.713	0.2073	0.620	4.1956	0.1669	0.919	0.0407	0.959
	TETR	0.2847	2.6028	0.565	0.0921	0.756	6.6282	0.0802	0.939	0.0470	0.913
	AMP	0.2951	1.9237	0.706	0.1842	0.702	4.3042	0.1502	0.946	0.0296	0.956
80	AMO	0.4105	2.7775	0.689	0.1842	0.668	4.6708	0.1455	0.940	0.0401	0.976
	TETR	0.3624	3.6886	0.512	0.0691	0.695	7.2409	0.0622	0.955	0.0560	0.911
	AMP	0.3753	2.6610	0.675	0.1612	0.724	4.6227	0.1312	0.945	0.0249	0.952
100	AMO	0.5095	3.6126	0.672	0.1612	0.672	4.9579	0.1351	0.934	0.0188	0.892
	TETR	0.4359	4.8564	0.468	0.0461	0.683	7.8903	0.0449	0.945	0.0460	0.958
	AMP	0.4576	3.6671	0.625	0.1382	0.749	5.3235	0.1063	0.960	0.0232	0.981

AMOX- Amoxicillin, TETRA – Tetracycline and AMP- Ampicillin

Table 4. Comparison and selection of the best diffusion model at different concentrations of the selected antibiotic mixture

Concentration (mg/L)	Weber-Morris	Matthew-Weber	Bangham	McKay
20	0.8596	0.6441	0.9256	0.9517
40	0.7104	0.6525	0.9152	0.9370
60	0.6617	0.6930	0.9348	0.9430
80	0.6261	0.6960	0.9470	0.9466
100	0.5888	0.7021	0.9467	0.9444
Average	**0.6893**	**0.6775**	**0.9339**	**0.9445**

3.3.3 Bangham Diffusion Model

The value of k_b increased from 1.6998, 2.8320 and 1.3986 mL/g/L for amoxicillin, tetracycline and ampicillin respectively to 4.9579, 7.8903 and 5.3235 (Table 3), as the concentration increased from 20 to 100 mg/L, their corresponding values of θ decreased from 0.3250, 0.2464 and 0.3562 to 0.1351, 0.0449 and 0.1063. The values of θ less than unity show that intraparticle diffusion or pore diffusion is one of the rates determining steps. However, the linearity of the Bangham plot suggests that adsorbate pore diffusion is not the only rate-controlling step (Amole et al., 2021).

3.3.4 McKay Film Diffusion Model

The McKay film constant, K_m were in the range of 0.0188-0.0407, 0.0421-0.0560 and 0.0203-0.029 mgg⁻¹min for amoxicillin, tetracycline and ampicillin, respectively, within the concentration range (20-100 mg/L) investigated (Table 3)

3.4 COMPARISON AND SELECTION OF THE BEST DIFFUSION MODEL

The McKay model plots showed the best fit of all the diffusion models investigated based on the average R^2 at different concentrations of the antibiotic mixture studied (Table 4). McKay diffusion model has the highest value (0.9445) while Matthew-Weber has the least (0.6779). The sequence of the selection of the mass transfer model based on average R^2 is McKay (0.9445) > Bangham (0.9339) > Weber-Morris (0.6893) > Matthew-Weber (0.6779).

4 CONCLUSION

The mass transfer rate of a multicomponent mixture of antibiotics adsorption onto activated carbon derived from the *Delonix Regia* pod has been investigated based on the existing mass transfer models. The amount of the antibiotics removed by the DRP-activated carbon increased as the initial concentration (20-100 mg/L) and time (10-240 mins) increased. The rate of uptake of the individual antibiotic is directly related to its molecular weight and this observation has not been reported in previous studies. The sequence of the selection of the mass transfer model based on average R^2 was McKay (0.9445) > Bangham (0.9339) > Weber-Morris (0.6893) > Matthew-Weber (0.6775). Suitable mass transfer of the adsorption, which was hardly studied in previous studies had been used to describe the adsorption of antibiotic mixture unto DRPAC developed. This development has given more insight into the required parameter needed in the design of an adsorption system for the treatment of wastewater containing antibiotics using activated carbon derived from waste biomass such as *Delonix Regia* pods. Other diffusion models such as the Furusawa-Smith method and film mass-transfer model may be considered in future studies.

REFERENCES

Amole, A.R., Araromi, D.O., Alade, A.O., Afolabi, T.J., & Adeyi, V.A. (2021). Biosorptive removal of nitrophenol from aqueous solution using ZnCl2-modified groundnut shell: optimization, equilibrium, kinetic, and thermodynamic studies. *International Journal of Environmental Science and Technology, 18*(10), 1859–1876.

Amuda, O.S., Adebisi, S.A., Adejumo, A.L., Olayiwola, A.O., & Farombi, A.G. (2015). Equilibrium, Kinetic and Thermodynamic Studies of Adsorption of Aniline Blue from Aqueous Media Using Steam-Activated Carbon Prepared from *Delonix regia* Pod. *Journal of Water Resource and Protection, 7*(1), 1221-1233.

Azarpira, H., Balarak, D., Joghatayi, A., & Mostafapour, F. K. (2019). Biosorption of Amoxicillin from Contaminated Water onto Palm Bark Biomass. *International Journal of Life Science and Pharmaceutical Research, 7*(1), 9-16.

Barbooti, M. M., & Zahraw, S. H. (2020). Removal of Amoxicillin from Water by Adsorption on Water Treatment Residues. *Baghdad Science Journal, 17*(3), 1071-1079.

Benjelloun, M., Miyah, Y., Gulsun, A.E., Zerrouq, F., & Lairini, S. (2021). Recent Advances in Adsorption Kinetic Models: Their Application to Dye Types. *Arabian Journal of Chemistry, 14*(1), 1-24.

Dada, A.O., Latona, D.F., Ojediran, O.J., & Osazuwa, O.N. (2016). Adsorption of Cu (II) onto Bamboo Supported Manganese (BS-Mn) Nanocomposite: Effect of Operational Parameters, Kinetic, Isotherms, and Thermodynamic Studies. *Journal of Applied Sciences and Environmental Management, 20*(2), 409 –422.

Dada, E.O., Ojo, I.A., Alade, A.O., Afolabi, T. J., Amuda, O.S., & Jameel, A.T. (2020). Biosorption of Bromophenol Blue from Aqueous Solution Using Flamboyant (*Delonix regia*) Pod. *Chemical Science International Journal, 29*(5), 32-50.

George, Z.K., Jie, F., & Kostas, A.M. (2014). New Biosorbent Materials: Selectivity and Bioengineering Insights. *Processes, 2*(8), 419-440.

Mashkour, M.S. (2012). Decolorization of Bromophenolblue Dye Under UV- Radiation with ZnO as Catalyst. *Iraqi National Journal of Chemistry, 46*(5), 189-198.

Mohammed, K., Riadh, B., Noureddine, N., Seif El Islam, L., Fayçal, D., Riad, L., Mohamed, T., Hamed B.H., Atef el Jery, Ahmed, A.A., and Lotfi, K., (2022). Pharmaceutical pollutants adsorption onto activated carbon: isotherm, kinetic investigations and DFT modeling approaches. *Comptes Rendus Chimie*1878-1543, https://doi.org/10.5802/crchim.161

Rahmanian, O., Heidari, M., & Jafari, K. (2018). Wastewater treatment for Amoxicillin removal using magnetic adsorbent synthesized by ultrasound process. *Ultrasonics - Sonochemistry, 45*, 248–256.

Ravichandran, P., Sugumaran, P., Seshadri, S., & Basta, A.H. (2018). Optimizing the route for production of activated carbon from Casuarina equisetifoliafruit waste. *Royal Society of Chemistry, 5*(9), 1-12.

Revellame, E.D., Fortela, D.L., Wayne, S., Rafael, H., & Zappi, M.E. (2020). Adsorption kinetic modeling using pseudo-first order and pseudo-second order rate laws: A review. *Cleaner Engineering and Technology, 1*(8), 1-13.

Seshadri, S., Sugumaran, P., Priya, S. V., & Ravichandran, P. (2012). Production and Characterization of Activated Carbon from Banana Empty Fruit Bunch and *Delonix regia* Fruit Pod. *Journal of Sustainable Energy & Environment, 3*(9), 125-132.

Supriyadi, D., Darmansyah, A., Farhani, C., Sanjaya, A., & Soraya, F. (2019). Evaluation of kinetics adsorption models from Lampung ethnic textile industry wastewater for removal of chromium onto modified activated sludge and zeolite adsorbent. *Conference Series: Earth and Environmental Science, 25*(8), 1-13.